Desalination and Water Treatment
www.deswater.com

doi: 10.1080/19443994.2012.760112

51 (2013) 5792–5804
August

Taylor & Francis
Taylor & Francis Group

Adsorption of Direct Blend Yellow D-3RNL onto bamboo-base activated carbon: optimization, kinetics, and isotherm

Lianggui Wang

School of Sciences, Lishui University, Lishui 323000, P.R. China
Tel. +86 578 2271250; email: wlgui@lsu.edu.cn

Received 20 October 2012; Accepted 13 December 2012

ABSTRACT

Adsorption of Direct Blend Yellow D-3RNL in aqueous solution by activated carbons prepared from *Moso* timber bamboo stem residues was optimized by using central composite design matrix and response surface methodology. A maximum dye removal from the experimental validation reached 92.1% under the optimum conditions (initial dye concentration 20 mg L^{-1}, pH 2, bamboo-based activated carbon dosage 20 g L^{-1}, temperature 50°C, and time of adsorption 20 h) with the relative standard deviation 5.37%. The high R^2 value (0.9487) for the second-order model obtained from the analysis of variance (ANOVA) indicated that the experimental data fitted well with the predicted data. The adsorption followed the nonlinear model of pseudo-second-order reaction and agreed well with Freundlich judged by the levels of Akaike Information Criterion and Akaike weight. Furthermore, the thermodynamics analysis indicated that the adsorption was a spontaneous, endothermic, entropy-increasing, and chemisorption process.

Keywords: Response surface methodology; Adsorption; Direct Blend Yellow D-3RNL; Bamboo-base activated carbon; Akaike Information Criterion; Kinetics; Isotherm

1. Introduction

Direct dyes, also called substantive dyes, are one of the most popular types of colorant used for the dyeing and printing of cellulosic fibers and their blends. Owing to the ease of their application and the wide gamut of colors available at a modest cost, direct dyes are still a popular dye class. Chemically, direct dyes are generally large molecules, containing two or more azo groups and sulfonic groups which provide solubility in water. Although the forces of attraction between the direct dyes and cellulose fibers may include hydrogen bonding, dipolar forces, and nonspecific hydrophobic interactions which are highly dependent upon the nature of the dye structure and the polarity of the dye molecule, 5–30% of direct dyes used may be lost to the effluent during such dying process [1] due to the fact that these dye molecules are attracted by physical forces at the molecular level to the textile. Thus, treatment of the effluents containing azo direct dye has become a great concern due to their color and potential toxicity to animals and humans alike [2,3]. At present, there are many processes available for the color removal from textile effluents by biodegradation [4,5], advanced oxidation processes [6–8] and biological oxidation [9], electrochemical and photoelectrochemical degradation [10–12], coagulation/flocculation [13–15], membrane separation [16], and adsorption processes [17–23]. However, most of the methods described

above require substantial financial input and their use is restricted because of cost factors overriding the importance of pollution control. In comparison with other techniques, adsorption is one of the most effective physical processes for the removal of dyes from wastewater stream because of its simplicity of design, ease of operation, and insensitivity to toxic substances. But, the high cost of the production and regeneration of adsorbent has restricted its use in industrial application. Therefore, recently activated carbons derived from agriculture waste/byproducts have been extensively explored for the treatment of the textile dye effluent [24–27].

Moso Timber Bamboo (*Phyllostachys heterocycla* cv. *pubescens*), a fast-growing and renewable grass, is very rich natural resources in Lishui City of Zhejiang Province of China. Thus, when *Moso* Timber Bamboo attains its maturity within five years, it is often used as raw materials to manufacture many items such as building material, kitchen implement, clothing, decorative items, furniture, toys, gifts, and a lot more. But, how to dispose of the bamboo residues from these plants remains a problem at present. *Moso* Timber Bamboo stem is an excellent material to prepare charcoal due to the fact that it contains high carbon content (48.64%) and low amounts of nitrogen (0.14%), sulfur (0.11%), and hydrogen (6.75%) [28]. Moreover, bamboo-based activated carbon has a large amount of micropores and an extremely large surface area, about 4 and 10 times greater than those in wood charcoal, respectively [29], and has been used as the potential commercially available adsorbent for the treatment of heavy metal ions [30–32], ammonia [33], and organic pollutants [34–38]. Direct Blend Yellow D-3RNL is an important direct blend dyestuff and is widely used in one bath one step dyeing process. Hence, it is necessary to develop a practical approach to treatment of wastewater containing this dye.

A classic and conventional optimization of process parameters was done by changing one variable at a time while keeping all others at constant level. This approach is not only time consuming, requires lots of experiments and could not depict the interactive effects of process variable, but also results in unreliable conclusions. However, response surface methodology (RSM) is a collection of mathematical and statistical techniques that uses quantitative data from appropriate experiments to determine regression model equations and operating conditions which are useful for developing, improving, and optimizing processes and can be used to evaluate the relative significance of some factors even in the presence of complex interactions [39,40]. So, in this work, a standard RSM design called a central composite design (CCD) is applied to optimize the adsorption of Direct Blend Yellow D-3RNL onto the bamboo-based active carbons from aqueous effluent. A detailed kinetic and equilibrium study of the Direct Blend Yellow D-3RNL removal with the bamboo-based active carbons has been made to understand the adsorption mechanism.

2. Materials and methods

2.1. Adsorbate and adsorbents

Direct Blend Yellow D-3RNL dye (98.5% purity, $C_{68}H_{48}O_{26}N_{16}S_8Na_8$, λ_{max} 412 nm), supplied by Zhejiang Runtu Co., Ltd (Zhejiang, China), was selected as the adsorbate without further purification. Fig. 1 shows the chemical structure of the dye. Double-distilled water was used to prepare the desired concentration of the dye solution. A spectrophotometer (UV-2401, Shimadzu) was employed to measure the dye concentration at λ_{max} using a standard calibration curve. The photometric analysis demonstrates that the λ_{max} of the studied dye molecule is insensitive to changes in solution pH.

The *Moso* Timber Bamboo stem residues collected from a toy plant was got rid of dust particles, dried in sunlight for 2–3 days, cut into small grains sized 0.5–3 mm, soaked in a concentrated HNO_3 solution at 25°C for 2 days with the assistance of ultrasonication, filtered, and then dried in the sun. Next, the mixture was put into a ceramic crucible in a tube furnace and carbonized at 500°C under flowing nitrogen (0.1 $m^3 h^{-1}$) for 3 h. The activated product was then cooled to room temperature under nitrogen, refluxed in alcohol, and washed with hot distilled water in an ultrasonic bath until the pH of the washing solution reached 6–7. After drying at 110°C in a vacuum drying oven for 4 h, the

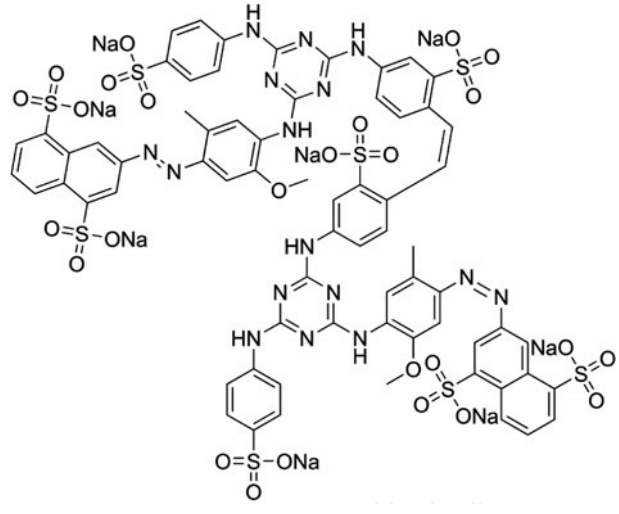

Fig. 1. Chemical structure of Direct Blend Yellow D-3RNL.

obtained bamboo-activated carbon (BAC) was sieved to obtain a size range of 0.15–0.25 mm and stored in a vacuum desiccator for further use.

The Brunauer–Emmett–Teller (BET) surface area (S_{BET}) of the prepared BAC was measured using nitrogen adsorption isotherms with a BET equation surface area analyzer (Micrometrics ASAP® 2020, USA). The total pore volume was defined as the volume of liquid nitrogen corresponding to the amount adsorbed at a relative pressure of $P/P_0 = 0.99$. Scanning electron microscopy (SEM) analysis was conducted to study the surface texture of the BAC and the development of porosity. The surface functional groups containing oxygen on BAC were determined by Boehm titration [41]. One gram of BAC sample was placed in 50 mL of the following solutions, each at a concentration of 0.05 mol L^{-1}: sodium hydroxide, sodium carbonate, sodium bicarbonate, and hydrochloric acidly. The vials were degassed under high purity nitrogen, sealed and shaken for 2 days to reach equilibrium, and then filtered. Five millilitre filtrate was pipetted, and the excess base or acid was titrated with 0.05 mol L^{-1} hydrochloric acid or sodium hydroxide, respectively. The number of basic sites was calculated from the amount of hydrochloric acid that reacted with the carbon. Each experiment was performed in triplicate under identical experimental conditions. The pHpzc value was determined by a mass titration method proposed by Noh and Schwarz [42]. BAC ranging 100–600 mg was taken. Each sample was placed in a 50-mL glass flask and 10 mL of sodium chloride (0.1 mol L^{-1}) was added. The flasks were sealed and stirred, and room temperature was maintained at 25˚C for 48 h to achieve equilibrium in the carbon charges. After 48 hours, the pH of each solution was measured with a PHS-3E pH-meter.

2.2. Batch adsorption experiments

Batch adsorption of Direct Blend Yellow D-3RNL dye onto the prepared BAC was carried out in triplicate. For each experiment, 50 mL dye solution of known concentration, known pH, and a known amount of the adsorbent was placed in a 150-mL Erlenmeyer flask. Similar procedure was followed for another containing the same dye concentration without adsorbent to be used as a blank. The mixture was agitated in a thermostat-controlled shaking water bath (Taicang Laboratorial Equipment Co., Ltd, China) at a constant speed of 180 rpm until the equilibrium was attained. Samples were withdrawn at appropriate time intervals and centrifuged at 3,600 rpm for 10 min. Subsequently, an aliquot of the supernatant was used for determination of the remaining dye concentration at its λ_{max}. The percentage of removal of the dyes and the amount of dye taken up by the adsorbent was calculated by applying Eqs. (1) and (2):

$$\%\ \text{Removal} = \frac{c_i - c_t}{c_i} \times 100 \quad (1)$$

$$q = \frac{(c_i - c_t).V}{m} \quad (2)$$

where c_i and c_t (mg L^{-1})are the liquid-phase concentrations of Direct Blend Yellow D-3RNL dye at initial and time t, respectively; q is the amount of dye adsorbed on the adsorbent at any time (mg g^{-1}), m (g) the mass of the adsorbent sample used, and V the volume of the dye solution (L).

2.3. Effect of pH on the adsorption

The pH of the adsorption system plays an important role in the adsorption largely due to its influence on the surface characteristics of the adsorbent and ionization/dissociation of the adsorbate molecule. The pH of the adsorption system is a relatively independent variable and the interaction seldom exists between it and other factors involved. Therefore, preliminary experiments were conducted to determine the optimal initial pH prior to designing the experimental runs. Experiments were carried out by varying the initial pH of the dye solution ranging between 2 and 9 while holding all the other relevant factors fixed at a specific set of conditions (an initial dye concentrations 30 mg L^{-1}, an activated carbon dosage 10 g L^{-1}, contact time 26 h, and temperature 40˚C). The pH value of the initial dye solution was adjusted using a 1 M HCl or NaOH solution.

2.4. Design of experiments

CCD is suitable for fitting a quadratic surface and helps to optimize the effective parameters with a minimum number of experiments as well as to analyze the interaction between the parameters. Generally, the CCD consists of a 2^n factorial runs with $2n$ axial runs and n_0 number of center points (six replicates). The contact time (X_1), temperature (X_2), initial dye concentration (X_3), and BAC dosage (X_4) were chosen as the independent variables. The range of values of the parameters was set using the results of the preliminary studies and the codes that correspond to these parameters were resolved.

A 2^4 factorial design was determined from CCD with the dye removal (Y, %) as an output depended

on four independent variables at five levels, consisting of 16 factorial points, 8 axial points and 6 replicates at the center points were employed, indicating that the total number of experiments with four variables was 30 ($=2^l+2l+6$), where l is the number of independent variables. The center points were used to determine the experimental error and the reproducibility of the data. The independent variables are coded where the low and high levels are represented as −2 and +2, respectively. The axial points are located at (±α, 0, 0), (0, ±α, 0) and (0, 0, ±α) where α is the distance of the axial point from center. In this study, the α value was fixed at 2 (rotatable). Thirty experiments were conducted in duplicate and average values were used for further calculations.

As we know, different variables are usually expressed in different units and/or have different limits of variation; the significance of their effects on response can only be compared after they are coded. For statistical calculations, the variable X_i was coded as x_i according to the following equation:

$$x_i = \frac{X_i - X_0}{\Delta X_i} \tag{3}$$

where x_i is the dimensionless coded value of the ith independent variable, X_i is the uncoded value of the ith independent variable, X_0 is the value of X_i at the center point, and ΔX_i is the step change value of the real variable i.

The sequence for the experimental work was randomly established to limit the influence of systematic errors on the interpretation of results. Table 1 shows the four controllable variables (factors) and their levels in coded and actual values. The output response is the dye removal (%) determined by Eq. (1). Each response was used to develop an empirical model which correlated the response to the dye adsorption variables using a second-degree polynomial equation as given by the following equation:

$$Y = b_0 + \sum_{i=1}^{n} b_i x_i + \sum_{i=1}^{n} b_{ii} x_i^2 + \sum_{i=1}^{n-1} \sum_{j=i+1}^{n} b_{ij} x_i x_j \tag{4}$$

where Y is the predicted response (dye removal efficiency), b_0 the constant coefficient, b_i the linear coefficients, b_{ii} the quadratic coefficients, b_{ij} the interaction coefficients, and x_i and x_j are the coded values of the adsorption variables.

Design-Expert software (version 8.0.5b, Stat-Ease, Inc., Minneapolis, USA) was employed to analyze the adsorption data. Analysis of variance (ANOVA) was performed and three-dimensional (3D) response surface curves were plotted to see the interaction between various independent parameters. The significance of each variable (factor) was determined using Student's t-test.

2.5. Kinetic and equilibrium models

The nonlinear regression usually involves the minimization or maximization of error distribution (between the experimental data and the predicted isotherm) based on its convergence criteria. Thus, regarding the adsorption kinetics and adsorption isotherms, five nonlinear kinetic equations (Avrami–Erofeev, Elovich, pseudo-first-order, pseudo-second–order, and intra-particle diffusion in Table 2) were applied to identify the key process controlling the adsorption rate; furthermore, six nonlinear isotherm equations listed in Table 2 (Langmuir, Freundlich, Temkin, Khan, Koble–Corrigan, and Redlich–Peterson) were used to stimulate and evaluate the experimental equilibrium data. The kinetic and equilibrium models were fit employing the nonlinear method. Moreover, these models were evaluated using the nonlinear coefficients of determination, the small-sample-corrected *Akaike* Information Criterion (AICc), and the the *Akaike* weight (w_i). The AICc is calculated for each model from the equation [43]:

$$\mathrm{AICc} = -n\ln\left(\frac{RSS}{n}\right) + 2p + \frac{2p(p+1)}{n-p-1} \tag{5}$$

where n is the number of experiments performed and p is the number of parameter of the fitted model. RSS is the residual sum of squared deviations (between

Table 1
The variables and values used for CCD

Variables	Coded factors	Coded factor levels					Step change values
		−2	−1	0	1	2	
Contact time (h)	X_1	6	11	16	21	26	5
Adsorption temperature (°C)	X_2	20	30	40	50	60	10
Initial dye concentration (mg L^{-1})	X_3	10	20	30	40	50	10
BAC dosage (g L^{-1})	X_4	5	10	15	20	25	5

Table 2
Nonlinear equations of the kinetic and isothermal models

Kinetic models	Nonlinear equations	Isothermal models	Nonlinear equations
Avrami–Erofeev	$q_t = q_e[1 - \exp(-k_{av} \cdot t)^n]$	Langmuir	$q_e = q_m \cdot k_L \cdot C_e/(1 + k_L \cdot C)$
Elovich	$q_t = 1/\beta \cdot [\ln(\alpha \cdot \beta) + \ln(t)]$	Freundlich	$q_e = k_F \cdot C^{n}_{F}$
Pseudo-first-order	$q_t = q_e[1 - \exp(-k_1 \cdot t)]$	Temkin	$q_e = (R \cdot T/b_T)\ln(k_T \cdot C_e)$
Pseudo-second-order	$q_t = k_2 \cdot t \cdot {q_e}^2/(1 + k_2 \cdot t \cdot q_e)$	Khan	$q_e = q_m \cdot k_K \cdot C_e/(1 + k_K \cdot C_e)^{n}_{K}$
	$h_0 = k_2 \cdot {q_e}^2$	Koble–Corrigan	$q_e = q_m \cdot k_{KC} \cdot {C_e}^{n}_{KC}/(1 + k_{KC} \cdot C^{n}_{KC})$
	Initial sorption rate		
Intra-particle diffusion	$q_t = k_{dif} \cdot t^{0.5} + I$	Redlich–Peterson	$q_e = a \cdot k_{RP} \cdot C_e/(1 + k_{RP} \cdot C^{n}_{RP})$

the measurement and the fitted curve). The *Akaike* weight can be expressed as:

$$w_i = \frac{\exp(-\Delta_i/2)}{\sum_{i=1}^{R} \exp(-\Delta_i/2)} \quad (6)$$

where $\Delta_i = \mathrm{AIC}_i - \mathrm{minAIC}$. The model with the smallest value of AICc and the largest w_i is estimated to be "closest" to reality (unknown but approximated by the model) among the candidate models considered.

3. Results and discussion

3.1. Characterization of BAC

Table 3 lists the physicochemical properties of BAC. It is apparent that the amount of the total acid groups is more than that of the total basic groups on the BAC surface. Similar results have been reported by Huang et al. [44]. This is due to the strong oxidizing character of nitric acid, so it can oxidize carbon atoms and cause the carbon surfaces to lose electrons and get positive charges. The SEM image of BAC (Fig. 2) displays many large regular and orderly pores on the surface.

3.2. Effect of initial solution pH

Understanding of the effect of pH on the adsorption process is helpful to determine the optimized operational parameters for application and to reveal the adsorption mechanism. The effect of the initial dye solution pH on the adsorption of Direct Blend Yellow D-3RNL dye onto BAC was evaluated within the pH range between 2 and 9 (Fig. 3). Fig. 3 shows that the dye removal efficiency decreased significantly with increasing pH, especially between pH 2 and 3.

The dissolved Direct Blend Yellow D-3RNL dye is negatively charged in aqueous solution, because it possesses eight sulfonic groups. The adsorption of this dye takes place when the adsorbents maintain a net positive charge when the solution pH is lower than pH_{pzc}. As a result, an electrostatic interaction occurs between the negatively charged dye molecules and the positively charged adsorption sites of the adsorbent. But, as the pH of the system increases beyond pH_{pzc}, the number of negatively charged sites on the adsorbents increases, which weakens the electrostatic attraction or even increases the electrostatic repulsion between the adsorbent surface and the dye molecules. This led to the decrease of the dye removal. In addition, the abundance of OH^- ions competing with the negatively charged dye molecules for the adsorption sites is also responsible for the lower dye removal percentages at higher pH. Similar results had been reported by Nevine [45] and Safa and Bhatti [46]. Thus, the following experiments were performed at pH 2.

3.3. Optimization of dye adsorption by RSM

The 4-factor CCD matrix and experimental results acquired in the adsorption runs are presented in Table 4. Based on Eq. (4), Table 5 shows the results of ANOVA on experimental results by the Design-Expert 8.0.5b. The significance of each term was determined

Table 3
Physicochemical properties of BAC

Apparent density ($g\,cm^{-3}$)	Ash content (% wt)	pH_{PZC}	S_{BET} ($m^2\,g^{-1}$)	Total pore volume ($cm^3\,g^{-1}$)	Total acid groups ($mmol\,g^{-1}$)	Basic groups ($mmol\,g^{-1}$)
0.61	6.4	6.79	451.2	0.31	0.562	0.217

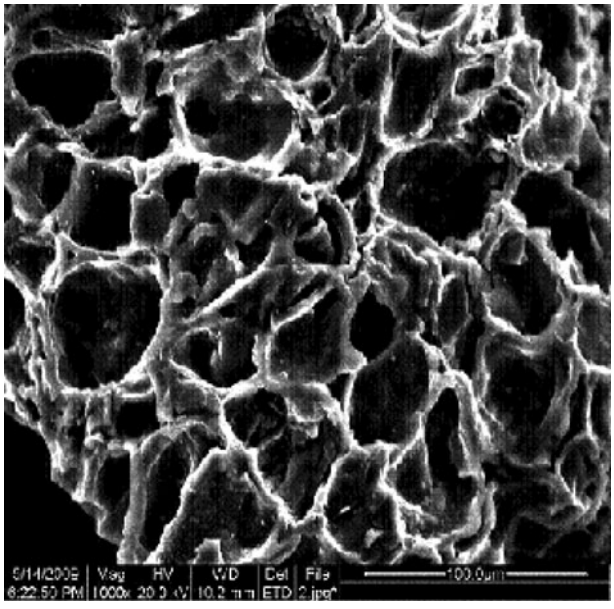

Fig. 2. SEM of BAC at 1,000×.

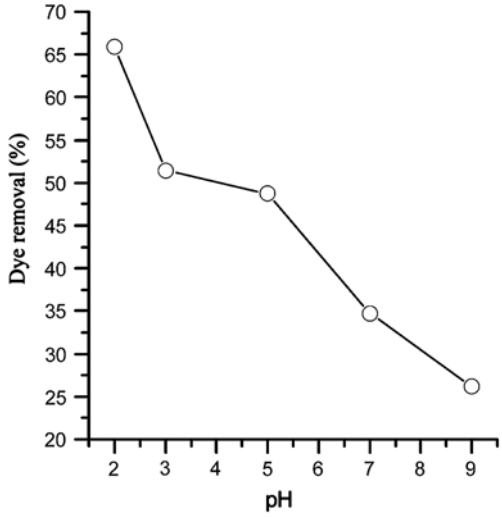

Fig. 3. Effect of the initial pH on the removal direct dye by BAC (initial dye concentration 30 mg L^{-1}, BAC dosage 10 g L^{-1}, contact time 20 h, and temperature 40°C).

using related *F*- and *p*-values. The variables with *t*-value higher than critical one (2.78 for linear and 2.12 for quadratic and interaction terms) and *p*-values < 0.05 have significant effect on the response. So, in this case, the variables X_1, X_2, X_3, X_4, X_1^2 and X_4^2 are significant in dye removal, whereas the other variables are not significant. As a result, Final Eq. (7) was developed by putting the significant terms in terms of actual factors as follows:

$$\text{Re}\ \% = -60.01 + 5.901X_1 + 0.5236X_2 - 0.902X_3 + 6.156X_4 - 0.155X_1^2 - 0.0916X_4^2 \quad (7)$$

In addition, on the basis of the coefficients in Eq. (7), the highest coefficient belonged to X_4 (BAC dosage), indicating that the BAC dosage exerted the greatest effect on the dye removal. Aber and Sheydaei [47] reported the similar result on the adsorption removal of Indigo dye onto activated carbon cloth.

The ANOVA of quadratic regression model shows that the model is highly significant, as it is evident from the Fisher's *F*-test with a very low probability value ($P_{\text{model}} > F$) = 0.0001) (Table 5). Relatively lower value of coefficient of variation (CV = 9.02% less than 10%) implies a better precision and reliability of the performed experiment [48]. The fit of the model to the data was evaluated by the determination of coefficients (R^2) and adjusted R^2 (R^2_{adj}) [49]. The high R^2 (0.9487) and relatively high R^2_{adj} (0.9353) value of the model indicate a close agreement between the experimental data and the predicted values from model. The value of R^2_{Pred} (0.8793) is in reasonable agreement with the R^2_{adj} value. Adequate precision ratio of 30.25 indicated an adequate signal, meaning that this model is desirable because the ratio is greater than four [50]. Chatterjee et al. [51] reported the similar result about the adsorption of methylene blue dye on a low-cost adsorbent prepared from *Parthenium hysterophorus* using RSM method. These results indicate the high precision in predicting the dye removal efficiency by BAC.

Fig. 4 shows the simultaneous effect of contact time and BAC dosage on the percentage adsorption of the direct dye at the fixed conditions: initial dye concentration 30 m g L^{-1}, pH 2, and temperature 40°C. It is clear that the dye removal efficiencies increased with the increasing of BAC dosage as well as batch contact time before 21 h. Increasing BAC dosage increases the number of active sites for the dye molecule and, therefore, it increases the removal of the dye. Prolonging the batch contact time before the equilibrium time provides sufficient chances for the interaction between adsorbent and dye. Combined effect of temperature and initial dye concentration was shown in Fig. 5. Lower initial dye concentration and higher temperature favored the dye removal efficiency.

Based on the above results, the batch contact time, the BAC dose, and system temperature all have the positive effect on the adsorption for the direct dye removal from aqueous solution, whereas the initial dye concentration has a slightly negative effect on the dye removal.

Table 4
List of experiments in the central composite design (uncoded values) for model optimization and the responses

Run no.	X_1	X_2	X_3	X_4	Re_{exp} (%)	$Re_{pred.}$ (%)	Residual (%)
1	16	20	30	15	52.24	49.94	2.30
2	21	30	40	20	55.88	61.78	−5.91
3	11	30	40	20	50.61	52.29	−1.69
4	21	50	40	20	73.95	72.26	1.69
5	16	60	30	15	76.12	70.88	5.24
6	16	40	10	15	87	78.44	8.56
7	16	40	30	15	59.25	60.41	−1.17
8	16	40	30	25	92.05	85.32	6.72
9	16	40	30	15	59.84	60.41	−0.58
10	11	30	40	10	18.58	18.22	0.36
11	11	50	20	20	76.13	80.79	−4.67
12	16	40	30	15	59.48	60.41	−0.94
13	11	50	20	10	42.47	46.72	−4.25
14	21	30	20	10	48.50	45.74	2.75
15	21	30	20	20	77.22	79.82	−2.60
16	11	50	40	20	59.02	62.76	−3.74
17	11	50	40	10	24.55	28.69	−4.14
18	26	40	30	15	58.52	54.43	4.09
19	11	30	20	10	30.21	36.25	−6.04
20	16	40	50	15	50.92	42.38	8.54
21	21	30	40	10	26.72	27.71	−0.99
22	16	40	30	15	59.48	60.41	−0.94
23	16	40	30	5	20.75	17.18	3.57
24	16	40	30	15	61.29	60.41	0.87
25	21	50	20	20	86.99	90.29	−3.30
26	16	40	30	15	59.11	60.41	−1.30
27	11	30	20	20	71.79	70.32	1.46
28	21	50	40	10	37.03	38.18	−1.15
29	6	40	30	15	41.65	35.44	6.20
30	21	50	20	10	52.24	56.22	−3.97

Optimization of the direct dye removal was performed by a multiple response method called desirability function to optimize different combinations of process parameters such as contact time, initial dye concentration, BAC dose, and temperature. For four variables, the criteria of the optimization were set in range. The importance for the goal was set to three plusses. The optimum conditions for maximum removal of the direct dye from aqueous solution were as follows: BAC dosage 20 g L^{-1}, initial dye concentration 20 mg L^{-1}, system temperature 50 ℃, and contact time 20 h. A maximum dye removal of 90.8% was obtained using the adsorption of the dye under optimum conditions with a desirability of 0.984, demonstrating that the estimated function represented the experimental model and desired conditions. Five confirmatory experiments were conducted on the predicted response obtained from the Design-Expert 8.0.5b application to check the alliance and its suitability. The average dye removal for the adsorption of the direct dye on BAC was 92.11% with the value of relative standard deviation (5.37%).

3.4. Adsorption studies

The adsorption performance of BAC under the optimized condition was evaluated through batch experiments, such as isotherms and kinetics, in order to confirm the degree of RSM fixation.

3.4.1. Kinetics of adsorption

The adsorption kinetics is significant in the treatment of wastewater and provides valuable insight into the reaction pathways and mechanisms of the

Table 5
ANOVA results for the selected quadratic mode for the dye removal by BAC

Source	Sum of squares	df	Mean square	*F*-value	*P*-value Prob > *F*	Significant
Model	10,746.29	14	767.59	24.48	<0.0001	Significant
X_1	540.08	1	540.80	17.25	0.0008	
X_2	658.02	1	658.02	20.99	0.0004	
X_3	1,950.85	1	1,950.85	62.22	<0.0001	
X_4	6,965.75	1	6,965.75	222.16	<0.0001	
X_1X_2	15.84	1	15.84	0.51	0.4882	
X_1X_3	4.53	1	4.53	0.14	0.7092	
X_1X_4	18.48	1	18.48	0.59	0.4546	
X_2X_3	19.48	1	19.48	0.62	0.4428	
X_2X_4	11.08	1	11.08	0.35	0.5611	
X_3X_4	7.73	1	7.73	0.25	0.6268	
X_1^2	392.87	1	392.87	12.53	0.0030	
X_2^2	1.87	1	1.87	0.06	0.8106	
X_3^2	23.95	1	23.95	0.76	0.3960	
X_4^2	133.51	1	133.51	4.26	0.0227	
Residual	470.32	15	31.35			
Lack of fit	467.15	10	46.72	73.61	<0.0001	Significant
Pure error	3.17	5	0.63	3.17		
Cor Total	11,216.62	29				

$R^2 = 0.9487$, $R_{adj}^2 = 0.9353$, $R_{Pred}^2 = 0.8793$, CV% = 92, adeq precision = 30.25.

adsorption reactions. Table 6 shows the parameter fits and the results. Based on their R^2 values, the five kinetic models studied fit the experimental data well for BAC in the following order of quality of fit: Avrami–Erofeev > pseudo-second-order > Elovich equation >pseudo-first-order > intra-particle diffusion. However, judged by the smallest AIC_c and the largest w_i, the adsorption kinetics of BAC were well described, and the quality of the fit followed the order of: pseudo-first-order > pseudo-second-order > intra-particle diffusion > Elovich equation > Avrami–Erofeev empirical model. There exists quite difference between the results above due to the different judgment standards. Comparing the $q_{e,cal}$ values of pseudo-first-order and pseudo-second-order models above with $q_{e,exp}$ value, the $q_{e,cal}$ value of pseudo-second-order model agrees very well with the $q_{e,exp}$ value, indicating that the pseudo-second-order kinetic model was the best of the five kinetic models to successfully describe the adsorption of the direct dye removal from aqueous phase by BAC. Similar kinetic results were also observed in the adsorption of indigo carmine on rice husk ash [52], the removal of the textile dye direct blue 78 on the polyaniline salts [53], and sorption of methylene blue and methyl violet onto mansonia wood sawdust [54]. The best fit to the pseudo-second-order kinetics implies that the adsorption mechanism depends on the adsorbate and adsorbent. At pH 2, there exist many protonated groups such as carboxylic group (–CO–OH_2^+), phenolic (–OH_2^+) and chromenic groups on the surface of the activated carbon [55]. Meanwhile, the direct dye molecule was partly or fully dissociated into large anion and sodium ion. Thus, large anion reacted with the protonated groups on the surface of the activated carbon.

Chemical reaction-based kinetic models successfully predicted the adsorption behavior of the direct dye onto BAC; however, these models do not reflect the importance of diffusion. Thus, to find out the role of diffusion in the process of dye adsorption, the intra-particle diffusion model was used to verify the influence of mass transfer resistance on the binding of the direct dye to BAC (Fig. 6). In Fig. 6, the curve was divided into three sections; the first, the sharpest stage, within 1 h, was attributed to the diffusion of the direct dye molecules through the bulk solution to the external surface of BAC or the boundary layer diffusion of the dye molecules. The second sharper stage from 1.5 to 18 h, described the gradual adsorption, where intra-particle diffusion was rate limiting and the third stage was attributed to the final equilibrium for which the intra-particle diffusion started to slow down due to extremely low dye concentration left in solution. The three stages in the plot suggest that the

Table 6
Parameters of the kinetic and isothermal models for the direct dye adsorption onto BAC

Kinetic models	Parameters	Isothermal models	Parameters
Elovich equation		Langmuir	
α ($mg\,g^{-1}\,min^{-1}$)	0.1507	q_m ($mg\,g^{-1}$)	1.5308
β ($g\,mg^{-1}$)	5.0923	k_L ($L\,mg^{-1}$)	0.1991
AICc	90.008	AICc	52.539
w_i	1.1×10^{-8}	w_i	0.0003
R^2	0.9863	R^2	0.9959
Pseudo-first-order		Freundlich	
k_1 (min^{-1})	0.0141	k_F ($mg^{1-n}\,L^n\,g^{-1}$)	0.3832
q_{cal} ($mg\,g^{-1}$)	1.2568	n_F	0.3787
AICc	53.202	AICc	36.543
w_i	0.9943	w_i	0.9846
R^2	0.7675	R^2	0.9423
Pseudo-second-order		Temkin	
K_2 ($gmg^{-1}\,min^{-1}$)	0.0162	b_T ($KJ\,mol^{-1}$)	7909.4
q_{cal} ($mg\,g^{-1}$)	1.3438	k_T ($mg\,L^{-1}$)	2.2197
h_0 ($mg\,g^{-1}\,min^{-1}$)	0.0292	AICc	44.904
AICc	63.765	w_i	0.0151
w_i	0.0051	R^2	0.9857
R^2	0.8968	Khan	
Intra-particle diffusion		q_m ($mg\,g^{-1}$)	2.0256
k_{dif} ($mg\,g^{-1}\,min^{-1}$)	0.0242	k_K ($L\,mg^{-1}$)	0.1368
I	0.5269	n_K	1.1410
AICc	67.984	AICc	64.648
w_i	0.0006	w_i	7.8×10^{-7}
R^2	0.9254	R^2	0.9972
Avrami–Erofeev equation		Koble–Corrigan	
q_{cal} ($mg\,g^{-1}$)	1.6946	q_m ($mg\,g^{-1}$)	1.5112
k_{av} (min^{-1})	0.1346	k_{KC} ($L^n\,mg^{-n}$)	0.1972
n_{av}	0.3488	n_{KC}	1.0259
AICc	102.29	AICc	62.646
w_i	2.2×10^{-11}	w_i	2.1×10^{-6}
R^2	0.9930	R^2	0.9961
Experimental uptake		Redlich–Peterson	
q_{exp} ($mg\,g^{-1}$)	1.3848	a ($L\,g^{-1}$)	1.9303
		k_{RP} ($L^n\,mg^{-n}$)	0.1422
		n_{RPn}	1.0662
		AICc	63.904
		w_i	1.1×10^{-6}
		R^2	0.9968

adsorption process occurs by surface adsorption and intra-particle diffusion (meso- and micropores).

3.4.2. Adsorption isotherms

Equilibrium data, commonly known as adsorption isotherms, are basic requirements for the design of adsorption systems. In order to understand the adsorption capacity of BAC, the equilibrium data were evaluated according to the six nonlinear isotherm models (Table 2). The adsorption isotherm of was investigated at a pH of 2, a dose of BAC of $20\,g\,L^{-1}$, a contact time of 20 h, and system temperature 30°C while varying the initial direct dye concentration ranging 5–70 $mg\,L^{-1}$ at a constant speed of 180 rpm. Table 6 lists the results of the equilibrium

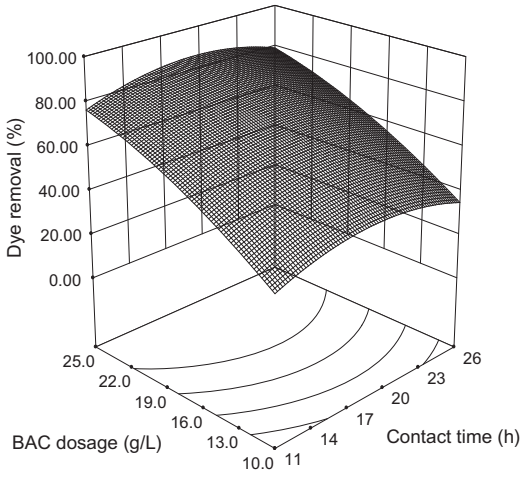

Fig. 4. Combined effect of BAC dosage and batch contact time on the percentage removal of the direct dye (pH 2, initial dye concentration 30 mg L^{-1}, and temperature 40°C).

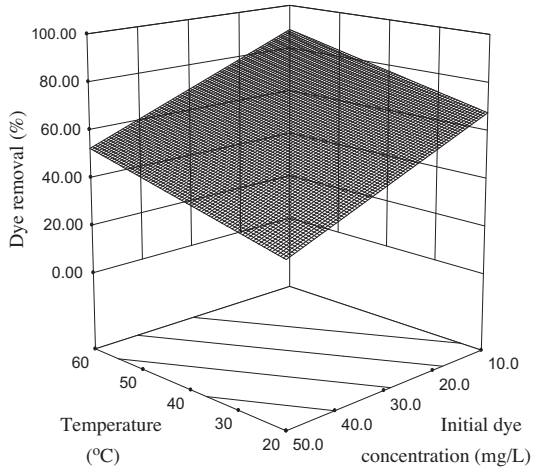

Fig. 5. Response surface 3D plot showing the effect of temperature and initial dye concentration on the removal efficiency (BAC dosage 15 g L^{-1}, batch contact time 1–6 h, and pH 2).

isotherm models for the adsorption of the direct dye onto BAC under the above experimental conditions. With respect to R^2 (in descending order): Khan > Redlich–Peterson > Koble–Corrigan > Langmuir > Temkin > Freundlich. It is also obvious that the three-parameter models give better fitting than the two-parameter models. However, according to the minimum value of AIC_c and the maximum value of w_i, the Freundlich model of the six isothermal models fits best to the experimental data. Furthermore, these results imply that the conventional two-parameter adsorption isotherm equations are still better models for describing the adsorption experimental isotherm data from the studied adsorption systems.

The Freundlich isotherm, an empirical equation, can be applied to nonideal adsorption on heterogeneous surfaces as well as multilayer adsorption. The n ($n = 1/n_F$) parameter, known as a measure of the adsorption intensity or the heterogeneity factor, can be used to indicate whether the adsorption is linear ($n = 1$), a chemical process ($n < 1$), or whether a physical process is favorable ($n > 1$); in contrast, the values of $n < 1$ and $n > 1$ indicate a normal Langmuir isotherm and cooperative adsorption, respectively [56]. In the present study, the value of n for BAC (0.3787) was less than unity, implying that the chemical process and the normal Langmuir isotherm were favorable.

3.5. Thermodynamic study

Thermodynamic study was carried out at initial dye concentration 20 mg L^{-1}, pH 2, BAC dosage 20 g L^{-1}, and a contact time of 20 h while varying system temperature from 20 to 60°C at a constant speed of 180 rpm. Thermodynamic parameters for adsorption of the direct dye onto BAC were undertaken from 20 to 60°C. Thermodynamic parameters, i.e. the change in free energy (ΔG°), the change in enthalpy (ΔH°), and the change in entropy (ΔS°), were calculated to evaluate the thermodynamic feasibility and the spontaneous nature of the process. ΔG°, ΔH°, and ΔS° were calculated using Eqs. (8)–(10).

$$k_d = \frac{C_{Ae}}{C_e} \tag{8}$$

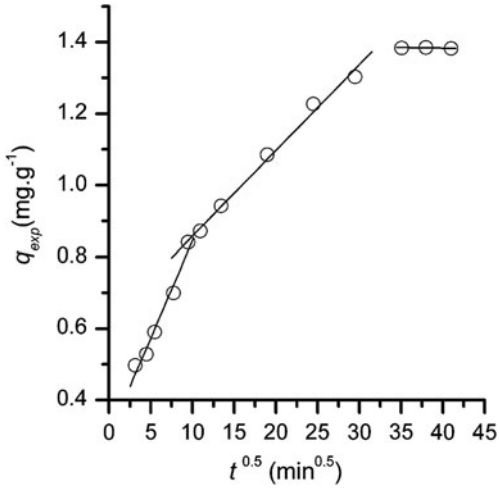

Fig. 6. Intra-particle diffusion model for the adsorption of the direct dye onto BAC (initial pH 2, initial dye concentration 30 mg L^{-1}, BAC dosage 15 g·L^{-1}, and temperature 40°C).

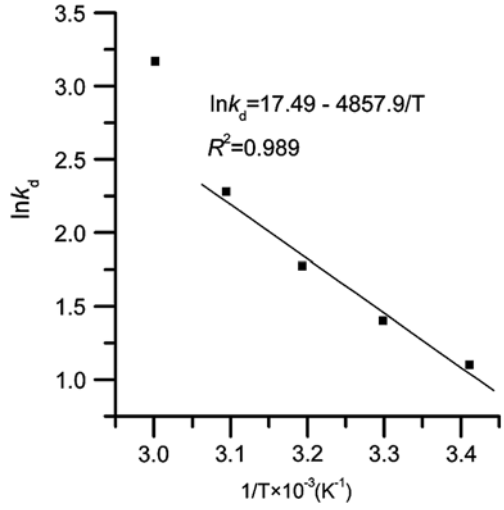

Fig. 7. Plot of ln k_d vs. $1/T$ for the adsorption of the direct dye on BAC (initial dye concentration 20 mg L^{-1}, initial pH 2, BAC dosage 20 g L^{-1}, and contact time 20 h).

$$\Delta G^{\circ} = -RT \ln k_d \quad (9)$$

$$\ln k_d = \frac{\Delta S^{\circ}}{R} - \frac{\Delta H^{\circ}}{RT} \quad (10)$$

where C_{Ae} (mg L^{-1}) is the equilibrium concentration adsorbed on adsorbent, C_e (mg L^{-1}) is the equilibrium concentration of adsorbate in bulk solution, T is the solution temperature in Kelvin, k_d is the equilibrium constant, and R is the gas constant (8.314 J mol^{-1} K^{-1}). ΔH° and ΔS° can be obtained from the slope and intercept of a Van't Hoff plot of lnk_d vs. $1/T$ (Fig. 7). Table 7 shows the negative values of ΔG° and positive ΔH° obtained indicated that the adsorption process is spontaneous and endothermic. The absolute values of ΔG° increase with the increase of temperature, which is in agreement with the isotherm and RSM results obtained in Section 3.3. The value of ΔH° was found to be 40.4 kJ mol^{-1}, slightly more than 40 kJ mol^{-1}, which further confirms the endothermic nature of the adsorption favorable at higher temperatures, possible strong bonding between dye and each adsorbent, and the possibility of chemical adsorption. The positive values of ΔS° suggest that there was increased randomness at the solid/solution interface with some structural changes in the adsorbate and adsorbent and a good affinity of the adsorbent for the direct dye.

Table 7
Thermodynamic parameters for the direct dye adsorption onto BAC

T (K)	ΔG° (KJ mol^{-1})	ΔH° (KJ mol^{-1})	ΔS° (J $mosl^{-1}$ K^{-1})
293.15	−2.680	40.38	153.7
303.15	−3.535		
313.15	−4.620		
323.15	−6.129		
333.15	−8.781		

4. Conclusion

Activated carbon prepared from *Moso* Timber Bamboo stem residues by chemical was used as an alternative adsorbent to remove Direct Blend Yellow D-3RNL from aqueous solutions. The result obtained from pH effect on the adsorption showed that lower pH favors the dye removal. RSM based on four-factor-five level Center Composite design was applied to explore the optimal conditions for the direct dye removal. The ANOVA showed that all the operating variables optimized, such as temperature, contact time, initial dye concentration, and adsorbent dosage, have the important impact on the adsorption, especially the adsorbent dosage. The high R^2 value for the model indicated that the actual data fitted well with the predicted data. The results attained from the model experimental validation revealed that 20 h of contact time was required to achieve 92.1% of the direct dye removal when the initial dye concentration, pH, BAC dosage, temperature, and shaking speed were 20 mg L^{-1}, 2, 20 g L^{-1}, 50 °C, and 180 rpm, respectively. The kinetic and isothermal data agreed well with the nonlinear types of pseudo-second-order model and Freundlich equation, repectively, judged by the levels of AICc and *Akaike* weight (w_i). The thermodynamic researches demonstrate that the adsorption is a spontaneous, endothermic, and chemisorption process.

Acknowledgements

This research was funded by the Educational Commission of Zhejiang Province of China with Project (No. Y201224951) and Public Welfare Technology Research Projects of Zhejiang Province (No. 2012C37038).

References

[1] J.K. Sharmaand, M.K. Arora, Environmental friendly processing for textile, Poll. Res. 20 (2001) 447–451.
[2] J.S. Bae, H.S. Freeman, Aquatic toxicity evaluation of new direct dyes to the Daphnia magna, Dyes Pigm. 73 (2007) 81–85.
[3] S.K. Dubey, A. Pandey, A.K. Bajaj, K. Misra, Some commercial azo dyes as inhibitors of mushroom tyrosinase DOPA oxidase activity, J. Pharmacol. Toxicol. 2 (2007) 718–724.

[4] A. Bafana, M. Jain, G. Agrawal, T. Chakrabarti, Bacterial reduction in genotoxicity of Direct Red 28 dye, Chemosphere 74 (2009) 1404–1406.
[5] C.R. Corso, E.J.R. Almeida, G.C. Santos, L.G. Morão, G.S.L. Fabris, E.K. Mitter, Bioremediation of direct dyes in simulated textile effluents by a paramorphogenic form of Aspergillus oryzae, Water Sci. Technol. 65 (2012) 1490–1495.
[6] G.S.Sergi, E.G. Abdellatif, F. Centellas, R.M. Rodríguez, C. Arias, J.A. Garrido, P.L. Cabot, E. Brillas, Comparative degradation of the diazo dye Direct Yellow 4 by electro-Fenton, photoelectro-Fenton and photo-assisted electro-Fenton, J. Electroanal. Chem. 681 (2012) 36–43.
[7] G.C. Collazzo, E.L. Foletto, L.J. Sérgio, M.A. Villetti, Degradation of Direct Black 38 dye under visible light and sunlight irradiation by N-doped anatase TiO_2 as photocatalyst, J. Environ. Manage. 98 (2012) 107–111.
[8] A. Filiz, E.C. Catalkaya, F. Kargi, A statistical experiment design approach for advanced oxidation of Direct Red azo-dye by photo-Fenton treatment, J. Hazard. Mater. 162 (2009) 230–236.
[9] M. Matto, Q. Husain, Decolorization of direct dyes by immobilized turnip peroxidase in batch and continuous processes, Ecotox. Environ. Safe. 72 (2009) 965–971.
[10] D. Vujevic, N. Koprivanac, A.L. Bozic, B.R. Locke, The removal of Direct Orange 39 by pulsed corona discharge from model wastewater, Environ. Technol. 25 (2004) 791–800.
[11] A. Socha, E. Sochocka, R. Podsiadły, J. Sokołowska, Electrochemical and photoelectrochemical degradation of direct dyes, Color. Technol. 122 (2006) 207–212.
[12] M.S. Morsi, A.A.A. Sarawy, W.A.S. El-Dein, Electrochemical degradation of some organic dyes by electrochemical oxidation on a Pb/PbO_2 electrode, Desalin. Water Treat. 26 (2011) 301–308.
[13] Y.F. Wang, B.Y. Gao, Q.Y. Yue, Y. Wang, Z.L. Yang, Removal of acid and direct dye by epichlorohydrin–dimethylamine: Flocculation performance and floc aggregation properties, Bioresour. Technol. 113 (2012) 265–271.
[14] B. Shi, G. Li, D. Wang, C. Feng, H. Tang, Removal of direct dyes by coagulation: The performance of performed polymeric aluminum species, J. Hazard. Mater. 143 (2007) 567–574.
[15] X.H. Xu, M.L. Li, Y. Yuan, Treatment of direct blending dye wastewater and recycling of dye sludge, Molecules 17 (2012) 2784–2795.
[16] H. Yoshida, T. Kataoka, M. Nango, S. Ohta, N. Kuroki, M. Maekawa, Transport of direct dye into cellulose membrane, J. Appl. Polym. Sci. 32 (1986) 4185–4196.
[17] S.V. Mohan, N.C. Rao, J. Karthikeyan, Adsorptive removal of direct azo dye from aqueous phase onto coal based sorbents: A kinetic and mechanistic study, J. Hazard. Mater. B90 (2002) 189–204.
[18] T.Z. Ren, Z.Y. Yuan, B.L. Su, Encapsulation of direct blue dye into mesoporous silica-based materials, Colloid Surf. A Physicochem. Eng. Asp. 300 (2007) 79–87.
[19] A.A. Ahmad, B.H. Hameed, N. Aziz, Adsorption of direct dye on palm ash: Kinetic and equilibrium modeling, J. Hazard. Mater. 141 (2007) 70–76.
[20] C.P. Kaushik, R. Tuteja, N. Kaushik, J.K. Sharma, Minimization of organic chemical load in direct dyes effluent using low cost adsorbents, Chem. Eng. J. 155 (2009) 234–240.
[21] Y. Safa, H.N. Bhatti, Adsorptive removal of direct textile dyes by low cost agricultural waste: Application of factorial design analysis, Chem. Eng. J. 167 (2011) 35–41.
[22] Y. Safa, H.N. Bhatti, Kinetic and thermodynamic modeling for the removal of Direct Red-31 and Direct Orange-26 dyes from aqueous solutions by rice husk, Desalination 272 (2011) 313–322.
[23] Y. Safa, H.N. Bhatti, Biosorption of Direct Red-31 and Direct Orange-26 dyes by rice husk: Application of factorial design analysis, Chem. Eng. Res. Des. 89 (2011) 2566–2574.
[24] C. Grégorio, Non-conventional low-cost adsorbents for dye removal: A review, Bioresour. Technol. 97 (2006) 1061–1085.
[25] V.K. Gupta, Suhas, Application of low-cost adsorbents for dye removal—a review, J. Environ. Manage. 90 (2009) 2313–2342.
[26] A. Bhatnagar, M. Sillanpää, Utilization of agro-industrial and municipal waste materials as potential adsorbents for water treatment—a review, Chem. Eng. J. 157 (2010) 277–296.
[27] M.A.M. Salleh, D.K. Mahmoud, W.A.W.A. Karim, A. Idris, Cationic and anionic dye adsorption by agricultural solid wastes: A comprehensive review, Desalination 280 (2011) 1–13.
[28] E.L.K. Mui, W.H. Cheung, V.K.C. Lee, G. McKay, Kinetic study on bamboo pyrolysis, Ind. Eng. Chem. Res. 47 (2008) 5710–5722.
[29] R.S. Zhao, J.P. Yuan, T. Jiang, J.B. Shi, C.G. Cheng, Application of bamboo charcoal as solid-phase extraction adsorbent for the determination of atrazine and simazine in environmental water samples by high-performance liquid chromatography–ultraviolet detector, Talanta 76 (2008) 956–959.
[30] S.Y. Wang, M.H. Tsai, S.F. Lo, M.J. Tsai, Effects of manufacturing conditions on the adsorption capacity of heavy metal ions by Makino bamboo charcoal, Bioresour. Technol. 99 (2008) 7027–7033.
[31] F.Y. Wang, H. Wang, J.W. Ma, Adsorption of cadmium (II) ions from aqueous solution by a new low-cost adsorbent-Bamboo charcoal, J. Hazard. Mater. 177 (2010) 300–306.
[32] H. Lalhruaitluanga, K. Jayaram, M.N.V. Prasad, K.K. Kumar, Lead (II) adsorption from aqueous solutions by raw and activated charcoals of Melocanna baccifera Roxburgh (bamboo)—a comparative study, J. Hazard. Mater. 175 (2010) 311–318.
[33] T. Asada, T. Ohkubo, K. Kawata, K. Oikawa, Ammonia adsorption on bamboo charcoal with acid treatment, J. Health Sci. 52 (2006) 585–589.
[34] E.L.K. Mui, W.H. Cheung, M. Valix, G. McKay, Dye adsorption onto char from bamboo, J. Hazard. Mater. 177 (2010) 1001–1005.
[35] B.H. Hameed, M.I. EI-Khaiary, Adsorption of methylene blue onto bamboo-based activated carbon: Kinetics and equilibrium studies, J. Hazard. Mater. 141 (2007) 819–825.
[36] A.A. Ahmad, B.H. Hameed, Fixed-bed adsorption of reactive azo dye onto granular activated carbon prepared from waste, J. Hazard. Mater. 175 (2010) 298–303.
[37] L.G. Wang, G.B. Yan, Adsorptive removal of direct yellow 161dye from aqueous solution using bamboo charcoals activated with different chemicals, Desalination 274 (2011) 81–90.
[38] L. Wang, Application of activated carbon derived from "waste" bamboo culms for the adsorption of azo disperse dye: Kinetic, equilibrium and thermodynamic studies, J. Environ. Manage. 102 (2012) 79–87.
[39] N. Bouchemal, Y. Azoudj, Z. Merzougui, Adsorption modeling of Orange G dye on mesoporous activated carbon prepared from Algerian date pits using experimental designs, Desalin. Water Treat. 45 (2012) 284–290.
[40] A.R. Khataee, G. Dehghan, E. Ebadi, M. Pourhassan, Central composite design optimization of biological dye removal in the presence of Macroalgae Chara sp, Clean—Soil Air Water 38 (2010) 750–757.
[41] H.P. Boehm, Some aspects of the surface chemistry of carbon blacks and other carbons, Carbon 32 (1994) 759–769.
[42] J.S. Noh, J.A. Schwarz, Estimation of the point of zero charge of simple oxides by mass titration, J. Colloid Interface Sci. 130 (1989) 157–164.
[43] C.F. Hurvich, C.L. Tsai, Regression and time series model selection in small samples, Biometrika 76 (1989) 297–307.
[44] G.L. Huang, J.X. Shi, T.A.G. Langrish, Removal of Cr (VI) from aqueous solution using activated carbon modified with nitric acid, Chem. Eng. J. 152 (2009) 434–439.

[45] A.K. Nevine, Removal of direct blue-106 dye from aqueous solution using new activated carbons developed from pomegranate peel: Adsorption equilibrium and kinetics, J. Hazard. Mater. 165 (2009) 52–62.
[46] Y. Safa, H.N. Bhatti, Kinetic and thermodynamic modeling for the removal of Direct Red-31 and Direct Orange-26 dyes from aqueous solutions by rice husk, Desalination 272 (2011) 313–322.
[47] S. Aber, M. Sheydaei, Removal of COD from industrial effluent containing indigo dye using adsorption method by activated carbon cloth: Optimization, kinetic, and isotherm studies, Clean—Soil Air Water 40 (2012) 87–94.
[48] K.T. Sirsalmath, C.V. Hiremath, S.T. Nandibewoor, Kinetic, mechanistic and spectral investigations of ruthenium (III)/osmium (VIII) catalyzed oxidation of paracetamol by alkaline diperiodatoargentate (III) (stopped flow technique), Appl. Catal. A: Gen. 305 (2006) 79–89.
[49] S. Weisberg, Applied Linear Regression, 2nd ed., Wiley, New York, NY, 1985.
[50] A. Mani, T. Kasinathan, S. Palanivel, Rapid removal of chromium from aqueous solution using novel prawn shell activated carbon, Chem. Eng. J. 186 (2012) 178–186.
[51] S. Chatterjee, A. Kumar, S. Basu, S. Dutta, Application of response surface methodology for methylene blue dye removal from aqueous solution using low cost adsorbent, Chem. Eng. J. 181 (2012) 289–299.
[52] U.R. Lakshmi, V.C. Srivastava, I.D. Mall, D.H. Lataye, Rice husk ash as an effective adsorbent: Evaluation of adsorptive characteristics for Indigo Carmine dye, J. Environ. Manage. 90 (2009) 710–720.
[53] A.S. Mohamed, The role of polyaniline salts in the removal of direct blue 78 from aqueous solution: A kinetic study, React. Funct. Polym. 70 (2010) 707–714.
[54] E.O. Augustine, Kinetic study and sorption mechanism of methylene blue and methyl violet onto mansonia (Mansonia altissima) wood sawdust, Chem. Eng. J. 143 (2008) 85–95.
[55] Y. Al–Degs, M.A.M. Khraisheh, S.J. Allen, M.N. Ahmad, Effect of carbon surface chemistry on the removal of reactive dyes from textile effluents, Water Res. 34 (2000) 927–935.
[56] K. Fytianos, E. Voudrias, E. Kokkalis, Sorption–desorption behavior of 2,4-dichlorophenol by marine sediments, Chemosphere 40 (2000) 3–6.